Research Paper

ARCHITECTURE OPTIMIZATION FOR NEURAL NETWORK BY ANALYZE THE PARAMETERS OF BEAM COLUMN JOINT

[1]Arul Gnanapragasam, [2]G.Chitra

Address for Correspondence

[1]Assistant Professor, Department of Civil Engineering, SSM Institute of Engineering and Technology, Dindigul, Tamilnadu

[2]Associate Professor, Department of Civil Engineering, Thiagarajar College of Engineering, Madurai, Tamilnadu, India

ABSTRACT

The expected performance of Reinforced Concrete (RC) beam column joints before and after being retrofitted using Fiber-Reinforced Polymer (FRP) composite materials is presented. Focus is given on the evaluation of the shear-strength versus deformation properties of the panel zone region either in the as-built or FRP-retrofitted configuration. Beam-column joint is used to analyze the performance in different specimens such as control, glass, basalt; hybrid (and rehabilitated specimen parameter are analyzed by use the Artificial Neural Network (ANN) with optimization process. Different optimization techniques are used optimize the hidden layer and neuron of the network architecture. The efficiency of a network can be increased if the volume of computation is reduced. That in neural network the output is related to the input via the weight of input to hidden layers and hidden to output layers. The optimal hidden layer and neuron attained in Social Spider Optimization (SSO) based predict the deflection of the beam column joint. The proposed work compared to the existing default structure and Genetic Algorithm (GA) the performance parameter is analyzed. All optimum results demonstrate that the attained error values between the output of the experimental values and the predicted values are closely equal to zero in the optimal network. From the results, the minimum error 90.146% is attained by optimal ANN structure with SSO algorithm compared to other techniques.

KEYWORDS: Fiber reinforced concrete, Beam column joint, hidden layer and neuron, Optimization technique, Deflection.

1. INTRODUCTION

In the current decades, it is not feasible to deliver the project containing the idea of sustainable development involving the employ of high performance, environment friendly materials generated at reasonable cost [1].Researchers as well try to generate high volume fly ash SCCs by replacing up to 60% of Portland cement with class F fly ash, achieving strength of about 40 Mpa [2]. Experimental investigation indicates also that joint deformation may significantly impact the global structural performance. Thus, it is necessary that inelastic joint action be simulated explicitly in predicting the response of reinforced concrete structures under earthquake loading [3]. Beam-column connections in reinforced concrete (RC) frame structures under earthquake-induced lateral displacements are generally subjected to large shear stresses that may lead to significant joint damage and loss of stiffness in the structure [4].The purpose of this study is to investigate the joint failure models for interior beam-to column joint. Tests of nine beam-to-column joint sub assemblages made of high strength reinforced concrete failed in joint shear are reexamined [5]. Shear forces in interior beam-column joints of typical moment resisting frames can be of the order of magnitude four to six times larger than the shear forces of the framing columns. This level of forces invariable leads to rather large shear stresses [6].General lack of ductility rather than inadequate lateral strength has been recognized as the fundamental source of deficiency in seismic performance of gravity load designed existing buildings, as a consequence of total absence of capacity design principles and poor reinforcement detailing [7]. Despite the number of experimental studies on the behavior of FRP retrofitted beam-column joints, relatively less work has been dedicated on the development of simple but reliable analysis and design procedure for FRP-strengthened joints [8].The performance of exterior joint assemblages designed for earthquake loads as per IS 1893:2002 are compared with the specimens having additional cross bracing bars provided on two faces of joint as confining reinforcements [9]. Thus, joint strength is a function of bond strength, and joint stiffness is a function of anchorage-zone deformation [10].The beam–column joints of SRC moment resisting frames (MRFs) bear significant shearing forces when subjected to earthquake type loading [11].The deep beam should be prepared with higher strength Self Compacting Concrete (HSSCC) for meeting the industry requirement which can be acquired by inserting fiber reinforced SCC (SCFRC) [12]. Several series of tests were conducted on reinforced concrete slab-beam-column sub assemblages in whom the participation of the slab in resisting the lateral load was investigated [13]. However, serious damage to beam–column joints began to appear due to seismic loads in the 60's [14].The application of fiber-reinforced polymer as a means of increasing the axial capacity of masonry columns made with clay bricks, through confinement was investigated [15].High strength, weight and stiffness to weight ratios and are chemically fairly inert, offering considerable potential for lightweight and durable retrofit [16]. These materials have higher ultimate strength and lower density than steel. The installation is easier and temporary support until the adhesive gains its strength is not required due to the low weight [17]. The FRP wrapping is triggered by the augmented lateral expansion of concrete when the latter approaches its ultimate strength, the yield moment and lateral stiffness of RC members are generally taken not to be influenced by that wrapping code [18].

2. LITERATURE REVIEW

In 2015 Rajagopal *et al* [19] have suggested the reinforced concrete structures, it was essential to enhance the performance of beam– column joints in moderate and severe seismic susceptibility areas. An attempt has been made to study and evaluate the performance of exterior beam–column joint using proper reinforcement anchorage. The anchorages are detailed as per ACI-352 (Mechanical anchorage), ACI-318 (90Standard bent anchorages) and IS-456

(Full anchorage) along with confinement. Significant improvements were observed in seismic performance, ductility and strength while used to hair-clip bar plus X-cross bar in combination with mechanical anchorage detail for higher seismic prone areas, apart from resolution to reducing congestion of reinforcement in joint core. The performances of anchorages and joint details, two groups of three specimens each were tested under reversal loading.

Fire behavior of FRP-strengthened reinforced concrete structural elements: A state-of-the-art review by Joao Firmo *et al* in 2015[20]. The paper presents a state-of-the-art review on the fire performance of FRP(fiber reinforced polymer)-strengthened RC structural elements. The review addresses first the mechanical behavior at high temperature of the constituent materials of FRPs and how their bond to concrete was affected when heated. Experimental and numerical studies on the fire behavior of FRP strengthened RC beams, slabs, and columns.

In 2014 Vijay Shankar *et al* [21] have proposed the beam-column joints, the lateral and vertical load resisting members in reinforced concrete structures, are particularly vulnerable to failures during earthquakes. Investigation of high performance concrete (HPC) joints with conventional concrete (CC) joints (exterior beam-column) was performed by comparing various reinforcement detailing schemes. Ten specimens are investigation and the results were compared: four specimens with CC (with and without seismic detailing), four specimens with HPC (with and without seismic detailing), and two Specimens with HPC at confinement joint. The test was conducted for lateral load displacement, hysteresis loop, load ratio, percent of initial stiffness versus displacement curve, total energy dissipation, strain in beam main bars, and crack pattern.

In 2014 Revathi *et al* [22] have seismic design philosophy, to ensure that the structure possesses at least a minimum strength to withstand minor earthquakes without damages and to resist moderate earthquakes without significant structural damages though some non structural damages may occur and to withstand major earthquakes without collapse. Among other things, the presence of slab has been observed to affect strength, stiffness and shear in the joint. Hence, an experimental study on beam-column joint with slab was necessary to understand the behavior of the slab. Two specimens with reduced scale were made to conduct experiments one with Beam-Column Joint with Slab (BCJS) and another with Beam-Column Joint without slab (BCJ).

Strength and behavior of steel plate–concrete wall structures using ordinary and eco-oriented cement concrete under axial compression by Byong- Jeong Choi *et al* 2014 [23] The main objectives of the study are to describe the compressive behavior and to determine the squash load of steel plate–concrete (SC) wall structures used ordinary and eco-oriented cement concrete. Six SC wall specimens were tested in compression in the test. In the three specimens, to reduce emissions of carbon dioxide (CO2), some of the cement in weight was replaced by the Hwangtho (red clay) which was traditional and environmental material. Based on the test results, simplified rule was suggested to evaluate the buckling stress for surface steel plate. Several comparisons were made to evaluate the predicted strengths and test results.

In 2012 Bayhan *et al* [24] have suggested the experimental and analytical study in reinforced concrete frames with weak beam-column joints. The beam-column connection did not contain transverse reinforcement that was typical in older-type construction. To our knowledge, no shaking table tests on frames failing in unreinforced beam-column joints have been reported. Linear and nonlinear analytical models based on the modeling procedures of ASCE/SEI 41 Supplement 1 were carried out and subjected to the input base motions. From the results are illustrate that the calculated response does not provide reasonably accurate values for the measured one.

Experimental Performance of Mortice and Tenon Joint Strengthened with Glass Fibre Reinforced Polymer under Tensile Load by Rohana Hassan *et al*, 2012 [25].The experimental performance of mortise and tenon joint for beam-to-column structural member made of Kempas species. The joints were dowelled with glass fibre reinforced polymer (GFRP) and compared to the joints strengthened with steel dowel and wood dowel. From the Results show that the experimental performance of the mortise and tenon joints dowelled with GFRP under tensile load may provide comparable strength to the joints dowelled with steel. Nevertheless, different behavior was shown in wood dowelled joints, the flexibility of wood dowels extended the displacement longer made the yield load and load at rapture extended compared to the other types of joints.

Comparative Study on Behavior of Reinforced Beam-Column Joints with Reference to Anchorage Detailing by Siva Chidambaram *et al* 2012 [26].The ductility capacity, energy dissipation capacity and load – deformation behavior of the exterior beam column joints constructed with an external anchorage system by providing a small projection beyond the column face was evaluated. The evaluation was based on the experimental results of two one fifth scale exterior bam column joint specimens tested as part of an extensive experimental program. A small axial load was applied to the column portion of the sub assembly and held constant during the test. From the test results indicate that external anchorage system exhibits excellent behavior in energy dissipation, ductility and load – deformation parameter than for specimens constructed to current design recommendations.

3. PROPOSED METHODOLOGY

The main objective of this proposed method is to develop the artificial model for evaluate the parameter of beam column joint. The evaluation parameter such as deflection, ductility and stiffness of the beam column joint by utilize the Feed Forward Back Propagation (FFBP) in Artificial Neural Network (ANN). Beam column area and the considerable properties of basalt and glass, which include the density, elongation, tensile strength and the young's modulus, which are analyzed based on the parameters such as the control specimen, glass specimen, basalt specimen, hybrid specimen and the rehabilitated specimens. In neural network the output is related to the input via the weight of input to hidden layers and hidden to output layers. Analysis purpose varying the hidden layers with optimization techniques, which are utilized to optimize the ANN structures to the various layers of beam column deflection value. For optimize these hidden layers and hidden neurons to increase

the efficiency of the neural network are using efficient training algorithm of the ANN process that is FFBN and different optimization technique which are Harmony search (HS) , Grey Wolf Optimization (GWO) and Social Spider Optimization(SSO). The number of layers and the number of processing elements per layer are important decisions. These parameters to a feed forward, back-propagation topology are also the most ethereal - they are the "art" of the network designer. The training process is repeated again to adapt the structure to the appropriate level important to foresee the yield.

Pseudo code for proposed method

Step 1: Structure initialization

{

Initialize the input ($I_i; i = 1,2,....6$) $I_i = \{X_1, X_2, Y_1, Y_2, V_X, V_Y\}$

Initialize the input layer weight $\{\alpha_i; i = 1,.....6 \text{ and } -10 \le \alpha \le 10\}$

Initialize the hidden layer weight $\beta_{ij}; j = 1,2....30 \text{ and } -10 \le \beta \le 10$

}

Number of hidden layer ($L = 5$)

Number of output layer ($O = 1$)

}

Step 2: Input layer

Basic function computation (B_f)

Step 3: Hidden layer

For optimizing Hidden layer and neuron by using SSO algorithm

Step 4: Social spider optimization algorithm

{

Initialize the weight hidden layers and neuron

Fitness computation (F_i) for (B_i)

Based on fitness update the New Spider population

Find the number of female and male spiders ($N_f \text{ and } N_m$)

Evaluate the weight (w_i) based on the fitness (F_i)

Fitness based initializes the population ($f_{i,j}^0 \text{ and } m_{k,j}^0$)

Find the Cooperative operator

Female cooperative operator (f_i^{t+1})

Male cooperative operator (m_i^{t+1})

Mating process find the probability (p_{si})

Find the fitness for the new Spider solution ($F_{i(new)}$)

}

Step 5: Store the best spider of the solution so for attained

Stop until optimal solution ($F_{optimal}$) attained

Iteration=Iteration+1

Step 6: Output layer

Obtain the basics function of the output layer unit (O_i)

Step 7: Find the error value (E_i)

3.1 Optimization on Artificial Neural Network Structure

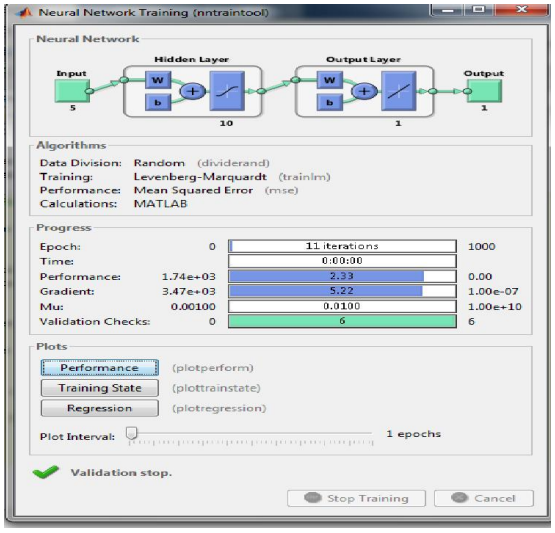

Fig 1 Architecture

In artificial neural network consists of a series of nodes (neurons) which have multiple connections with other nodes. Each connection has a weight associated with it which can be varied in strength, in analogy with neurobiology synapses. The principal with it which a neural network operates is relatively simple. Each neuron in the input layer holds a value, so that the input layer holds the input vector. Each of these neurons connects to every neuron in the next layer of neurons.

Figure 1 showed that the architecture model for he ANN structure this structure consists of input layer, output layer and hidden layers between these two layers. The number of these layers is dependent on the problem we are trying to solve, that is basically on the user. Our work is to optimize these hidden layers to increase the speed and efficiency of the neural network we are using. To optimize these hidden layers and neurons of the neural network, we have used another very recent and useful problem solving and optimization approach called social spider optimization (SSO).

3.2 Feed forward Back propagation network (FFBN)

In feed forward neural network, back propagation algorithm is computationally effective and works well with optimization and adaptive techniques, which makes it very attractive in dynamic nonlinear systems. The structure of a back-propagation ANN is shown in Figure2. The output of each neuron is the aggregation of the numbers of neurons of the previous level multiplied by its corresponding weights. The input values are converted into output signals with the calculations of activation functions. Back-propagation ANNs have been widely and successfully applied in diverse applications, such as pattern recognition, location selection and performance evaluations.

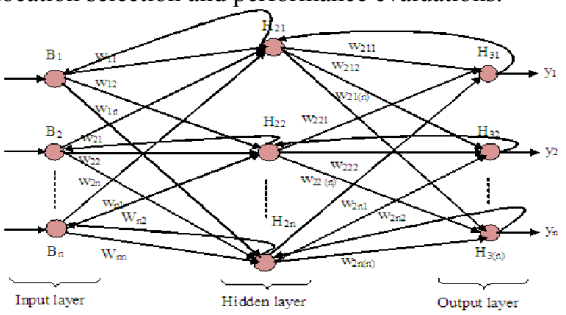

Fig 2 feed forward back propagation network

The SSO–BP is an optimization algorithm combining the SSO with the BP. The BP algorithm, on the contrary, has a strong ability to find local optimistic result, but its ability to find the global optimistic result is weak. By combining the SSO with the BP, The fundamental idea for this hybrid algorithm is that at the beginning stage of searching for the optimum, the SSO is employed to accelerate the training speed. When the fitness function value has not changed for some generations, or value changed is smaller than a predefined number, the searching process is switched to gradient descending searching according to this heuristic knowledge.

3.2.1 Structure initialization

Initialization process six inputs based the input layer weight α_j and the hidden layer weights β_{ij} are initialized Beam column joint input parameters B_i .Here considers the 5 hidden layers and neuron varying (1 to 30) and output layer is one.

3.2.2 Input layer

A vector of predictor variable values is presented to the input layer. The input layer distributes the values to each of the neurons in the first hidden layer. The input values and β is a weight of the input layer neuron, N is a number of data and B is a input values. In these value based calculate the basics function

$$B_f = \sum_{j=1}^{N} B_i \times \beta_{ij} \qquad (i = 1,2,...6) \qquad (1)$$

Where B_f is a basics function, β_{ij} is an input layer weight and i is a number of input $B_1 = \text{Density}$, $B_2 = \text{Elongation}$, $B_3 = \text{Area}$, $B_4 = \text{Tensile strength}$, $B_5 = \text{Young's modulus and } B_6 = \text{load}$.

3.2.3 Hidden layer with SSO process

A group of neurons between an input layer and output layer the outputs from the hidden layer are distributed to the output layer. The neurons of first hidden layer are directly connected to the input layer (data layer) of the neural network; Optimize the multi hidden layer and neuron of the network structure. The networks yield almost similar results with much reduced error so may claim to have reduced one of the hidden layers. Optimize the multilayered network to obtain the error rate of the each hidden layer by varying the neurons while achieving the minimum error rate value. Multi layer structure Calculate the outputs for the each hidden layer use the following equation. The outputs of the hidden layer $(i = 1, l2,...5)$

$$H_i = \begin{Bmatrix} H_i^1 \\ . \\ . \\ H_i^2 \\ . \\ . \\ H_i^n \end{Bmatrix} = \begin{Bmatrix} f(A_{f1}) \\ . \\ . \\ f(A_{f_2}) \\ . \\ . \\ f(A_{fn}) \end{Bmatrix}$$

The network can have any number of hidden layers. The values on the output layer of neurons are the outputs from the network. ANN structure obtains the optimal hidden layer and neuron different optimization technique is used. In this arithmetical demonstration social spider optimization (SSO) strategy is observed to achieve the optimal hidden layer and neuron of the evaluation process.

3.3 Social Spider Optimization (SSO)

The SSO assumes that entire search space is a communal web, where all the social-spiders interact to each other. In the proposed approach, each solution within the search space represents a spider position in the communal web. Every spider receives a weight according to the fitness value of the solution that is symbolized by the social-spider.

3.3.1 Initialization

Initialize the input parameters such as hidden layer and neuron is an initial solution spiders and i is a number of solutions this process is known as initialization process. The hidden layer and neuron is taken as the S_i that is

$$S_i = \{S_{0j}, S_{1j}, ...S_{nj}\}$$

Where S_i defines an initial solution, i ε [1, 2 … 5] and j ε [1, 2 … 30] since, i^{th} value is considered as the number of solution and j^{th} value is considered as length of solution.

3.3.2 Fitness function

Evaluate the fitness value of each solution and then calculate the best solution values.

$$F_i = \sum_{j=1}^{h} \alpha_j * \left(\frac{1}{1 + \exp(-\sum_{i=1}^{N} B_i \beta_{ij})} \right) \qquad (2)$$

Where, F_i is a fitness function α and β are weights, B is the input parameters, i is the number of inputs; j is the number of weights and h is the number of hidden neurons. Find the fitness for the each layer $(i = 1,2..5)$.Find the new solutions for the process update the new spiders.

3.3.3 New population Updation by using following procedure

The algorithm models two different search agents (spiders): males and females. Depending on gender, each individual is conducted by a set of different evolutionary operators which mimic different cooperative behaviors that are commonly assumed within the colony. Considering N as the total number of n-dimensional colony members, define the number of male N_m and females N_f spiders in the entire population S

$$N_f = floor[0.9 - rand.025).N] \quad and \quad N_m = N - N_f \qquad (3)$$

Where rand is a random number between [0, 1] and floor (.) maps a real number to an integer number.

3.3.4 Weight assignation

In the biological metaphor, the spider size is the characteristic that evaluates the individual capacity to perform better over its assigned tasks. Every individual (spider) receives a weight w_i which represents the solution quality that corresponds to the spider i (irrespective of gender) of the population S. Calculate the weight of every spider of S equation (4) is used.

$$w_i = \frac{F(s_i) - worst_S}{best_s - worst_s} \qquad (4)$$

Where $F(s_i)$ is the fitness value obtained by the evaluation of the spider position s_i with regard to the objective function F. The values $worst_s \; and \; best_s$ are calculated below equation

$$best_s = \min_{k=\{1,2,...N\}} (F(s_k)) \; and \quad worst_s = \max_{k=\{1,2,...N\}} (F(s_k)) \qquad (5)$$

3.3.5 Fitness based initializes the population

The algorithm begins by initializing the set S of N spider positions each spider position $f_i and \; m_i$ is a n dimensional vector containing the parameter values to be optimized. Such values are randomly and uniformly distributed between the pre specified lower initial parameter bound p_j^{low} and the upper initial parameter bound p_j^{high} just as it distributed by using equation(5) and (6).

$$f_{i,j}^0 = p_j^{low} + rand(0,1).(p_j^{high} - p_j^{low}) \quad (i = 1,2...N_m, j = 1,2,..n) \qquad (6)$$

$$m_{k,j}^0 = p_j^{low} + rand(0,1).(p_j^{high} - p_j^{low}) \quad (k = 1,2...N_m, j = 1,2,..n) \qquad (7)$$

Where $i, j \; and \; k$ are the parameter and individual indexes respectively whereas zero signals the initial population. Hence $f_{i,j}$ is the jth parameter of the ith female spider position.

3.3.6 Cooperative operators

3.3.6.1 Female cooperative operator

Female spiders present an attraction or dislike over others irrespective of gender. For a particular female spider, such attraction or dislike is commonly developed over other spiders according to their vibrations which are emitted over the communal web. Since vibrations depend on the weight and distance of the members which have originated them, strong vibrations are produced either by big spiders or other neighboring members lying nearby the individual perceives them. The first one involves the change in regard to the nearest member to i that holds a higher weight and produces the vibration $Vibc_i$.The second one considers the change regarding the best individual of the entire population S who produces the vibration $Vibb_i$. The female vibration $Vibc_i$ and $Vibb_i$ are calculated by using equation (8).

$$Vibc_i = w_c.e^{-d_{i,c}^2} \qquad Vibb_i = w_b.e^{-d_{i,b}^2} \quad (8)$$

The Vibration $Vibc_i$ are perceived by the individual $i(s_i)$ as a result of the information transmitted by the member $c(s_c)$ who is an individual that has two important characteristics: it is the nearest member to i and possesses a higher weight in comparison to $i(w_c > w_i)$. The Vibration $Vibb_i$ are perceived by the individual i as a result of the information transmitted by the member $b(s_b)$ with b being the individual holding the best weight that ids fitness of the entire population S such that $w_b = \max_{k\in\{1,2,...N\}} w(k)$.

If *rm* is smaller than threshold PF an attraction movement is generated; otherwise a repulsion movement is produced. Therefore, such operator can be modeled as follows:

$$f_i^{k+1} = \begin{cases} f_i^k + \alpha.Vibc_i.(s_c - f_i^k) + \beta.Vibb_i.(s_b - f_i^k) + \delta.(rand - 1/2) \text{ with } \text{proability } PF \\ f_i^k - \alpha.Vibc_i.(s_c - f_i^k) + \beta.Vibb_i.(s_b - f_i^k) + \delta.(rand - 1/2) \text{ with } \text{proability } 1-PF \end{cases} \quad (9)$$

Where α, β, δ *and* *rand* are random numbers between [0, 1] whereas k represents the iteration number. The individual s_c *and* s_b represent the nearest member to i that holds a higher weight and the best individual of the entire population S.

3.3.6.2 Male cooperative operator

Male members, with a weight value above the median value within the male population, are considered the dominant individuals D. On the other hand, those under the median value are labeled as non-dominant ND males. In order to implement such computation, the male population $M(M = \{m_1, m_2, ...m_{N_m}\})$ is arranged according to their weight value in decreasing order. Thus, the individual whose weight $w_{N_{f+m}}$ is located in the middle is considered the median male member the vibration of the male $Vibf_i$ calculated by using below equation (10). The Vibration $Vibf_i$ perceived by the individual $i(s_i)$ as a result of the information transmitted by the member $f(s_f)$ with f being the nearest female individual to i.

$$Vibf_i = w_f.e^{-d_{i,f}^2} \quad (10)$$

Since indexes of the male population M in regard to the entire population S are increased by the number of female members N_f, the median weight is indexed by N_{f+m}. According to this, change of positions for the male spider can be modeled as follows.

$$m_i^{k+1} = \begin{cases} m_i^k + \alpha.Vibf_i.(s_f - m_i^k) + \delta.(rand - 1/2) if \quad w_{N_{f+i}} > w_{N_{f+m}} \\ m_i^k + \alpha.\left(\frac{\sum_{h=1}^{N_m} m_h^k.w_{N_{f+h}}}{\sum_{h=1}^{N_m} w_{N_{f+h}}} - m_i^k\right) if \quad w_{N_{f+i}} \le w_{N_{f+m}} \end{cases} \quad (11)$$

Where the individual s_f represents the nearest female individual to the male member i whereas $\left(\sum_{h=1}^{N_m} m_h^k.w_{N_{f+h}} \Big/ \sum_{h=1}^{N_m} w_{N_{f+h}}\right)$ Correspond to the weighted mean of the male population M.

By using this operator, two different behaviors are produced. First, the set D of particles is attracted to others in order to provoke mating. Such behavior allows incorporating diversity into the population. Second, the set ND of particles is attracted to the weighted mean of the male population M. This fact is used to partially control the search process according to the average performance of a subgroup of the population.

3.3.7 Mating process

Mating in a social-spider colony is performed by dominant males and the female members. Under such circumstances, when a dominant male m_g spider ($g \in D$)locates a set E^g of female members within a specific range r(range of mating), it mates, forming a new brood s_{new} which is generated considering all the elements of the set T^g that, in turn, has been generated by the union $E^g \cup m_g$. It is important to emphasize that if the set E^g is empty, the mating operation is canceled. The range r is defined as a radius which depends on the size of the search space. Initialize randomly the female $(F = \{f_1, f_2, ...f_{N_f}\})$ and male $(M = \{m_1, m_2, ...m_{N_m}\})$ where $S = \{S_1 = f_1\ S_2 = f_2 .....S_{N_f} = f_{N_f}$, and $S_{N_{f+1}} = m_1, S_{N_{f+2}} = m_{2...} S_N = m_{N_m}\}$ calculate the radius mating.

$$r = \frac{\sum_{j=1}^{n} (p_j^{high} - p_j^{low})}{2.n} \quad (12)$$

In the mating process, the weight of each involved spider (elements of T^g) defines the probability of influence for each individual into the new brood. The spiders holding a heavier weight are more likely to influence the new product, while elements with lighter weight have a lower probability. The influence probability P_{si} of each member is assigned by the roulette method, which is defined as follows;

$$p_{si} = \frac{w_i}{\sum_{j\in T^k} w_j} \qquad where \quad i \in T^g \quad (13)$$

Once the new spider is formed, it is compared to the new spider candidate s_{new} holding the worst spider s_{wo} of the colony, according to their weight values. If the new spider is better than the worst spider, the worst spider is replaced by the new one. Otherwise, the new spider is discarded and the population does not suffer changes. In case of replacement, the new spider assumes the gender and index from the replaced spider. Such fact assures that the entire population S maintains the original rate between female and male members. These process based find the optimum hidden layer and neuron of the neural network process.

3.3.8 Optimal solution

Based on above mention process attain the optimal hidden layer and neuron also find the optimal fitness which is defined as $F_{optimal}$ in this optimal fitness based find the output. The optimal values based predict the output deflection of the Glass specimen, basalt specimen, control specimen, rehabilitated specimen and hybrid specimen of beam column joint.

$$F_{i(optimal)} = \sum_{j=1}^{h} \alpha_j * \left(\frac{1}{1+\exp(-\sum_{i=1}^{N} B_i \beta_{ij})} \right) \qquad (14)$$

3.4 Output layer

The output layer has a number of neurons. The hidden layer neurons are connected with the output layer by the neurons. Each connection has a weighted value such as $\alpha_1, \alpha_2, \ldots\ldots \alpha_n$.The basis function of the Output units is expressed by the Equation is O_l and the out is deflection of each specimen.

$$O_l = \sum_{i=1}^{n} \alpha_i \, \sigma(F_{i(optimal)}) \quad l = 1, i \in 1 \qquad (15)$$

The error value calculation the equation which is defined as E_i Where, α and β are weights range from -50 to 50,i is the number of inputs, j is the number of weights and h is the number of hidden neurons.

$$E_i = \sqrt{\frac{\sum_{i=1}^{ND} (D_i - P_i)^2}{ND}} \qquad (16)$$

Where ND is the number of the data, D is the desired value and P is the predicted value, i= 1,2,….n. By using this formula, the error value is getting from the difference between desired value and predicted value.

4. RESULT AND DISCUSSION

Proposed work the results are taken in working platform of MATLAB 2014 with the system configuration, i5 processors with 4GB RAM is used in ANN with optimization process. Then the performance of a beam column joint is evaluated then obtains the best specimen of the beam-column joint. Based on the experimental investigation held up for different specimen BFJC, BCJB, BCJG, BCJBG and rehabilitated specimens along with the load and fiber properties, in order to retrieve deflection for developing the optimal network structure attained in SSO technique. In further the differential error between realtime output and the attained output from Optimal ANN is found to be near equal to zero. Existing algorithm that is genetic algorithm (GA) and FFBN technique compared to proposed method and improve the accuracy.

4.1 Neural Network Structure for optimization techniques

Different optimization technique such as HS, GWO and SSO algorithm are used to obtain the optimal Hidden layer and neuron of the ANN shows the below table. Proposed structure compared to the existing process GA and default structure.

Table 1 Structure with Different optimization techniques

Technique	Structure	Error Accuracy (%)
SSO	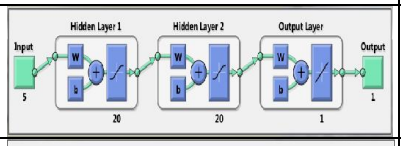	90.6
GWO	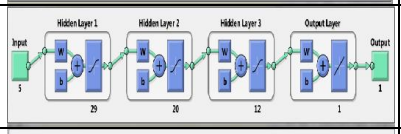	88.34
HS	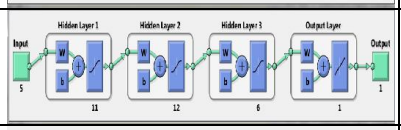	81.31
LM(FFBN)	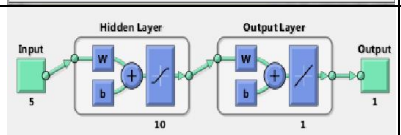	86.55
GA	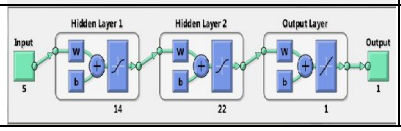	88.71

Table 1 shows that the All the optimization algorithm attained ANN structure and error accuracy the optimal structure attained in the SSO process. Neural network structure five hidden layer and neuron varying 1 to 30 the optimal structure of SSO having hidden layer one and hidden layer two with 20 neurons to produce the maximum error accuracy of deflection in beam column joint. Proposed SSO technique error accuracy compared to GWO and HS the difference is 57.76% and also compared to the existing process that is FFBN and GA is the difference is 27.53%.Existing technique the structure has Hidden layer one with 14 neurons and hidden layer 2 with 22 neuron the neuron and hidden layer based minimize the error value of deflection in beam column joint.

4.2 Convergence graph

The graph showing below successfully show the deflection of beam column joint fitness graphs based on iteration of the HS, GWO and SSO by altering the hidden layer and neuron and thus the error values are determined. The error graph is drawn with the iteration symbolized in the X-axis and fitness in the Y–axis.

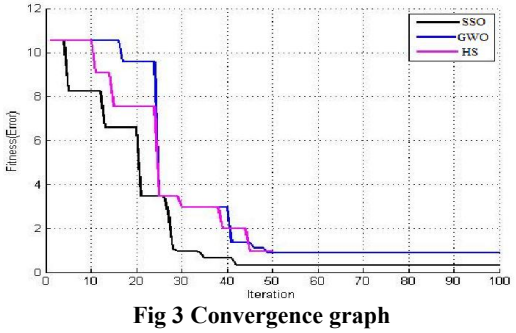

Fig 3 Convergence graph

Figure 3 shows that the convergence graphs for the ANN structure with optimization process average deflection error value of the beam column joint. This graph basically resolves that the SSO procedure is given minimum fitness in least iteration compared to existing work of beam column joint. Minimum error this work 1.08 attained in the 42th iteration it's compared to the GWO the error increased as 82% and HS is 74.54%.Proposed method initial iteration the average error value is 11.23 in 7th iteration. Then the iteration is varied the performance also changing in all techniques. The maximum fitness of HS is 11.3 after 13 iterations. Through the graph the lion algorithm Optimization strategy just specifies the ideal fitness value with the efficient results.

4.3 Experimental results and Predicted values for proposed method

Neural network process the testing results and original values for the beam column joint different specimens are shown in below table ANN with optimization technique the nearby value occur in SSO technique. The all the specimens consider the input the area of beam column joint is 17.5m. Table 2 and 3 shows the deflection of the control and rehabilitated specimen in beam column joint. If the load applied the deflection is varied the nearby deflection value occur in the SSO process. The load is 3 in two control specimens the actual deflection is 3.17 and 2.01 the predicted value is 3.20 and 2.65.The error difference of the BJC1 is 77.4% and BCJC2 is 68.23% similarly other values of control specimen.

Table 2 Deflection for Control specimen

BCJC1			BCJC2		
Input	Output(Deflection)		Input	Output(Deflection)	
Load	Actual value	SSO value	Load	Actual value	SSO value
2	2.02	1.794	2.5	1.45	1.884
3	3.17	3.203	3	2.01	2.65
5	7.75	7.075	3.5	2.74	2.062
7	12.83	12.83	5.5	5.47	7.76
10	20.05	21.990	7.5	11.55	13.428

Table 3 Deflection for Rehabilitated specimen

BCJR1			BCJR2		
Input	Output(Deflection)		Input	Output(Deflection)	
Load	Actual value	SSO value	Load	Actual value	SSO value
2	2.02	1.762	2	2.54	1.122
3	3.45	3.232	3	3.83	3.2032
5	6.42	7.07	6	11.41	9.460
7	11.49	12.41	10	25.48	22.38
10	20.34	20.99	12	30.17	25.81

In table 3 shows rehabilitated specimen also the nearby deflection is attained in the SSO process BCJR is an identical like a control specimen. For the load 10 the actual deflection is 20.34 in BCJR1 and 30.17 in BCJR2 the predicted value difference is 65% and 54.23% similar to the remaining load of rehabilitated specimen.

Table 4 Deflection for Glass specimen

Inputs(BCJG1& BCJG2)				BCJG1			BCJG2		
Density	Elongation	Tensile strength	Young's modulus	Load	Output(Deflection)		Load	Output(Deflection)	
					Actual value	SSO value		Actual value	SSO value
2.65	3.3	4200	105	2	1.12	1.35	3	2.79	2.596
2.65	3.3	4200	105	5	5.63	5.41	6	6.42	6.60
2.65	3.3	4200	105	11	14.28	13.28	11	11.19	13.21
2.65	3.3	4200	105	15	24.77	24.417	18	31.41	31.43
2.65	3.3	4200	105	17	26.07	31.49	18.3	39.89	39.224

Table 5 Deflection for Basalt specimen

BCJB						
Input					Output(Deflection)	
Load	Density	Elongation	Tensile strength	Young's modulus	Actual value	SSO value
4	2.5	2.5	3400	70	5.55	5.494
5	2.5	2.5	3400	70	6.71	7.089
9	2.5	2.5	3400	70	20.35	20.21
11	2.5	2.5	3400	70	28.35	28.45
12	2.5	2.5	3400	70	30.67	31.93

Fiber reinforced polymer concrete glass and basalt original deflection and simulation results are shown above tables. Table 4 two glass specimen results are shown if the load is 11 and the properties of the glass specimen consider as 2.65,3.3,4200,105 the deflection is 14.28 and predicted value is 13.28. BCJG2 also the deflection the proposed method compared to experimental process the difference is 63.048%.Then the basalt specimen also the deflection predicted value of the load 11 is 28.45 and the actual value is 28.35 if they load varied the deflection also changing. Glass and basalt specimen deflection value is nearby in SSO process.

Table 6 Deflection for Hybrid specimen

Inputs(BCJG1& BCJG2)							Output(Deflection)					
Load	Density		Elongation		Tensile strength		Young's modulus		BCJG1		BCJG2	
									Actual value	SSO value	Actual value	SSO value
	Glass	Basalt	Glass	Basalt	Glass	Basalt	Glass	Basalt				
2	2.65	2.5	3.3	2.5	4200	3400	105	70	0.96	0.96	1.98	1.98
3	2.65	2.5	3.3	2.5	4200	3400	105	70	1.77	1.77	3.16	3.16
7	2.65	2.5	3.3	2.5	4200	3400	105	70	10.65	10.64	16.41	16.41
10	2.65	2.5	3.3	2.5	4200	3400	105	70	19.33	19.33	24.91	24.9
11	2.65	2.5	3.3	2.5	4200	3400	105	70	22.31	20.3	27.13	27.88

Table 6 shows that hybrid specimen (basalt &glass) deflection value of the proposed method and experimental process. Here consider the properties density, elongation, tensile strength and young's modulus are taken the value combination of basalt and glass specimen. If the load 7 the deflection value is 0.96 for BCJBG1 and the predicted the similar value also and BCJBG2 has the deflection is 24.91 and the predicted value is 24.9.All the deflection for the load the minimum error attained in social spider optimization process.

4.4 Error values of deflection in all specimens

Different optimization techniques are compared to obtain the minimum error value of deflection in each specimen such as control (BCJC1, BCJC2), glass (BCJG1, BCJG2), basalt (BCJB), hybrid (BCJBG1, BCJBG2) and the rehabilitated (BCJB1, BCJB2).Hidden layer and neuron based the error value are calculated the minimum error value is attained in optimal structure of ANN process with SSO .

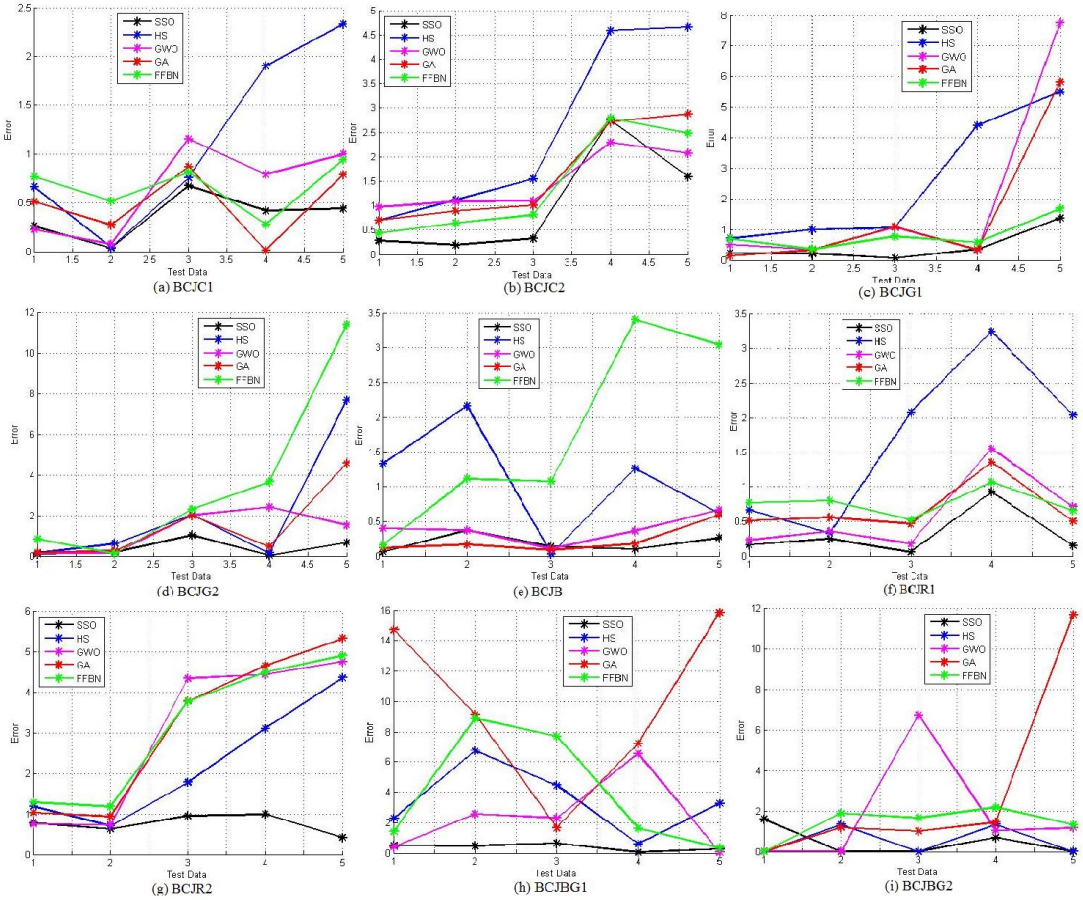

Fig: 4 Error Graph

Figure 4 shows that the error values of the all the specimens of the beam column joint testing data values. Figure (a) and (b) shows the control specimen error values the minimum error value of the Network structure attained in the SSO process minimum error value of BCJC1 is 0.50.Its compared to the HS the difference is 70.23% and GWO is 69.23%.BCJC2 also the proposed method compared to existing method the error differences is 96.45% totally the control specimen the error difference is low compared to other technique. Figure(c) and (d) shows the glass specimen deflection error values the initial testing data the predicted value error minimum in all techniques and the performance of the graph will be changed based on the objective function.FRP composite specimens all the testing data values minimum error of the proposed method is 96.25% compared to existing method. Figure (f) and (g) is rehabilitated specimen it's a control specimen failure in initial testing process BCJR1 the SSO error value of initial testing data is 0.112.This value is minimum compared to other techniques similar values attained in the BCJR2 also. Final figures show the hybrid specimen it's a combination glass ad basalt properties based deflection is varied. Deflection error value for the first hybrid specimen is 0.32 and specimen 2 is 0.318 it's a minimum of the specimen. All the specimens of beam column joint the minimum error value attained in the SSO process compared to optimization process and Existing work.

4.5 Ductility and Stiffness

The parameter such as Ductility and Stiffness of all specimens Experiment results compared to the simulation results of all specimens shows in below figure. These parameters are finding out by using below formulas in all specimens equation (17) and (18) ultimate load is a maximum load and yield deflection is a deflection for initial cracking load.

$$stiffness = \frac{Ultimate\ \ load}{Ultimate\ \ Deflection} \quad (17)$$

$$Ductility = \frac{Ultimate\ \ Deflection}{Yield\ \ Deflection} \quad (18)$$

Experimental results and SSO process results for each specimen stiffness and ductility showed that the figure (5).Figure (a) shows the stiffness for the all the specimens in control specimen BCJC1 and BCJC2 the stiffness value in real time experiment is 0.49 and when compared to the simulation the difference is 3% only and the FRP specimens also experimental and simulation value error also minimum. All the specimens the predicted stiffness value is 97% nearby value for experimental analysis.

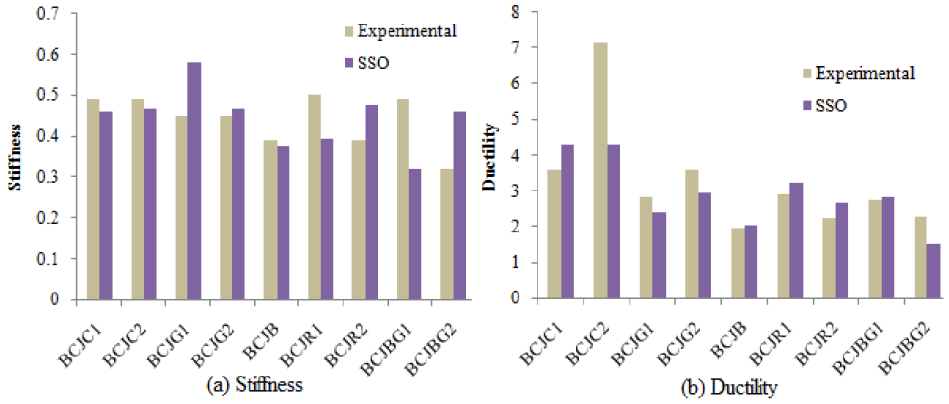

Fig 5 Comparison results in stiffness and ductility

Figure (b) shows the ductility value of the beam column joint for each specimen. Control specimen the actual value of ductility is 3.58 and 7.17 and predicted value is 4.28 for control specimen similar value occurs in all specimens.

5. CONCLUSION

Beam column joints for all specimens BCJC1, BCJC2, BCJG1, BCJG2, BCJB, BCJBG1, BCJBG2, BCJB1, BCJB2 predict the deflection, ductility and stiffness use the ANN with SSO process.SSO process attained the Optimal hidden layer and neuron of the ANN structure based on this structure predict the parameters. The convincing output results are observed to be nearly equal to the data set minimum error value achieved in the optimization method compared to existing work. Proposed method the error percentage of deflection in Control specimen, Glass specimen, basalt specimen, rehabilitated specimen and hybrid specimen is 85.45%, 92.25%, 97.65%, 87.69% and 87.69% of prediction process and stiffness and ductility is 81.82%,78.04%.This process compared to existing method GA the error minimized as 95.42%. In future the ANN investigators will look towards further unbelievable improvement methodologies for the produce of diminished errors with their excellent techniques for the Beam column joint.

REFERENCE

1. Dinakar ,Babu and Manu Santhanam, "Durability properties of high volume fly ash self compacting concretes, Journal of Cement & Concrete Composites,Vol.30,pp.880–886,2008.
2. Bouzoubaa and Lachemi , "self Compacting concrete incorporating high volumes of class F fly ash, Preliminary results", Journal of Cement concrete research,vol.31,No.3, pp413-420.,2001.
3. Nilanjan Mitra and Laura Lowes, "Evaluation and Advancement of a Reinforced Concrete Beam-Column Joint Model", In Proceedings of 3th World Conference on Earthquake Engineering,pp.1-11,Canada,2004.
4. Gustavo Parra-Montesinos, Sean Peterfreund, and Shih-Ho Chao,"Highly Damage Tolerant Beam-Column Joints Through Use of High-Performance Fiber-Reinforced Cement Composites, "Journal of ACI Structural,Vol.102,No.3,pp.487-495, 2005.
5. Shiohara Hitoshi, "Analysis of Joint Shear Failure Of High-Strength Reinforced Concrete Interior Beam-To-Column Joint", Journal High Strength Concrete. ASCE , pp.1-14, 1998.
6. Jose RESTREP And Cheng-Ming Lin, "Evaluation Of The Shear Strength Of Beam-Column Joints Of Reinforced Concrete Frames Subjected To Earthquake Loading", In proceedings 12th world conf. earthquake engineering,pp.1-8, 2000.
7. Pampanin, Calvi and Moratti, "Seismic Behaviour Of R.C. Beam-Column Joints Designed For Gravity Loads", In Proceedings of 12 the European Conference on Earthquake Engineering,pp.1-10,2002.
8. Umut Akguzel and Stefano Pampanin, "Assessment and Design Procedure for the Seismic Retrofit of Reinforced Concrete Beam-Column Joints using FRP Composite Materials" ,Journal of Composites for Construction,Vol.16,No.1,pp. 21-34,2012.
9. Syed Sohailuddin and Shaikh, "Finite Element Modeling Of Reinforced Concrete Beam Column Joint Using Ansys", Journal of structural and civil engineering research, Vol.2, No.3, pp.1-10,2013.
10. Laura Lowes and Arash Altoontash, "Modeling Reinforced-Concrete Beam-Column Joints Subjected to Cyclic Loading", Journal Of Structural Engineering, pp.1686-1697, 2003.
11. Cheng-Cheng Chen , Budi Suswanto and Yu-Jen Lin, "Behavior and strength of steel reinforced concrete beam–column joints with single-side force inputs",J ournal of Constructional Steel Research, Vol. 65,pp.1569–1581,2009.
12. Mohammad Mohammadhassani,Mohd Zamin Jummaat, Mohammed Jameel,Hamid Badiee and Arul Arumugam, "Ductility and Performance assessment of high strength self compacting (HSSCC)Deep beams: An Experimental Investigation", Nuclear Engineering and Design, Vol. 250,pp116-124, 2012.
13. Saddam Ahmed and Umarani Gunasekaran, "Testing and evaluation of reinforced concrete beam-column-slab joint", Journal of Gradevinar, Vol. 66,No .1,pp. 21-36,2014.
14. Jung-Yoon Lee, Jin-Young Kim and Gi-Jong Oh,"Strength deterioration of reinforced concrete beam–column joints subjected to cyclic loading",Journal of Engineering Structures,Vol.31,pp.2070–2085, 2009.
15. Francesco Micelli, Riccardo Angiuli ,Paolo Corvaglia and Antonietta Aiello,"Passive and SMA-activated confinement of circular masonry columns with basalt and glass fibers composites", Journal of Composites: Part B, Vol. 67,pp.348–362,2014.
16. Kazem Sharbatdar, Kheyroddin and Emami", cyclic performance of retrofitted reinforced concrete beam–column joints using steel prop", journal of Construction and Building Materials, Vol.36, pp. 287–294, 2012.
17. Tara Sen and .Jagannatha Reddy,"Finite Element Simulation of Retrofitting of RCC Beam Using Sisal Fibre Composite (Natural Fibre)",In proceedings of Electronics Computer Technology (ICECT), 2011 3rd Conference IEEE,Vol.6,pp.29-33,2011.
18. Rajagopal and Prabavathy, "Investigation on the seismic behavior of exterior beam–column joint using T-type mechanical anchorage with hair-clip bar", Journal of King Saud University-Engineering Sciences, Vol.27, pp.142-152, 2015.
19. Joao Firmo, Joao Correia and Luke Bisby, "Fire behavior of FRP-strengthened reinforced concrete structural elements: A state-of-the-art review", Journal of Composites Part B, Vol.80, pp.198- 216, 2015.
20. Vijay Shankar and Suji, "Seismic Behaviour of Exterior Reinforced Concrete Beam-Column Joints in High Performance Concrete Using Metakaolin and Partial Replacement with Quarry Dust "Journal of ISRN Materials Science,pp.1-12,2014.
21. Revathi and Risanthi, "Flexural Behavior of Corner Beam–Column Joint with and without Slab under Cyclic Loading in RC Framed Structures", Journal of Advanced Structures and Geotechnical Engineering,Vol.3,No.3,pp.1-5,2014.
22. Byong-Jeong Choi, Cheol-Kyu Kang and Ho-Young Park, "Strength and behavior of steel plate–concrete wall structures using ordinary and eco-oriented cement concrete under axial compression", Journal of Thin-Walled Structures,Vol.84,pp.313-324,2014.
23. Bayhan,Moehle,Yavari , Elwood,Lin, Wu and Hwang, "An Experimental and Analytical Study in Reinforced Concrete Frames with Weak Beam-Column Joints", In proceedings of 15th World Conference on Earthquake Engineering,pp.1-10,2012.
24. Experimental Performance of Mortice and Tenon Joint Strengthened with Glass Fibre Reinforced Polymer under Tensile Load, In proceedings of Business, Engineering and Industrial Applications (ISBEIA), IEEE Symposium,pp.856-860,2012.
25. Siva Chidambaram and Thirugnanam, "Comparative Study on Behavior of Reinforced Beam-Column Joints with Reference to Anchorage Detailing", Journal of Civil Engineering Research,Vol,Vol.2,No.4,pp.12-17,2012.